Journal of Applied Polymer Science

Functionalized Liquid Natural Rubber and Liquid Epoxidized Natural Rubber: A Promising Green Toughening Agent for Polyester

Hanieh Kargarzadeh,[1] Ishak Ahmad,[1] Ibrahim Abdullah,[1] Raju Thomas,[2] Alain Dufresne,[3] Sabu Thomas,[4] Aziz Hassan[5]

[1]Polymer Research Center (PORCE), School of Chemical Sciences and Food Technology, Faculty of Science and Technology, Universiti Kebangsan Malaysia (UKM), 43600 Bangi Selangor, Malaysia

[2]Department of Chemistry, Mar Thoma College, Tiruvalla 689103, Kerala, India

[3]The International School of Paper, Print Media and Biomaterials (Pagora), Grenoble Institute of Technology, CS10065—F-38402 Saint Martin d'HèresCedex, France

[4]Center for Nanoscience and Nanotechnology, School of Chemical Sciences, Mahatma Gandhi University, Priyadarshini Hills P. O., Kottayam, 686560 Kerala, India

[5]Department of Chemistry, Polymer and Composite Materials Research Laboratory, University of Malaya, Kuala Lumpur 50603, Malaysia

Correspondence to: I. Ahmad (E-mail: gading@ukm.edu.my) and H. kargarzadeh (E-mail: hanieh.kargar@gmail.com)

ABSTRACT: Toughened unsaturated polyester resins (UPRs) were prepared using two different reactive rubbers, namely, liquid natural rubber (LNR) and liquid epoxidized natural rubber (LENR). The effect of varying amounts of LNR and LENR on the morphology, thermal, and mechanical properties of UPR were evaluated. Fourier Transform Infrared spectroscopy was used to investigate the probable crosslinking reaction and changes in the functional groups on crosslinking. Field emission scanning electron microscopy and infinite focus microscopy were used to study the morphology of fracture surfaces. Tensile test showed that both the rubber-modified resins (1.5 wt %) improved tensile strength. The viscoelastic properties and thermal stability of the toughened polyesters were evaluated using dynamic mechanical thermal analysis and thermogravimetric analysis, respectively. A slight reduction in the glass transition temperature (T_g) of the polyester was reported on the addition of both the rubbers. An increment in impact strength and fracture toughness was observed at 1.5 wt % for LNR and 4.5 wt % for LENR-modified UPR. The results showed that both the liquid rubbers improved the mechanical properties of UPR. However, LENR-modified UPR exhibited a more significant improvement in the mechanical properties compared to LNR-modified UPR. © 2014 Wiley Periodicals, Inc. J. Appl. Polym. Sci. **2015**, *132*, 41292.

KEYWORDS: biopolymers and renewable polymers; blends; functionalization of polymers; polyesters; properties and characterization

Received 27 February 2014; accepted 10 July 2014

DOI: 10.1002/app.41292

INTRODUCTION

Unsaturated polyester resin (UPR) is one of the most popular thermosets that is used as a matrix in composites owing to its advantageous properties, such as high strength, modulus, and water resistance, as well as room temperature cure capability and transparency. However, UPR being brittle in nature needs to be modified by toughening agents at room and low temperature to fulfill some industrial requirements, such as marine and aerospace industries.

It is well known that the fracture toughness of thermoset materials can be improved using low-molecular-weight liquid rubbers.[1,2] In this technique, the liquid rubbers are initially dissolved into thermoset resins followed by separation of the rubber as a discrete particulate phase. This is due to the decreased solubility of the rubber in the matrix as a result of the increase in the molecular weight of the resin on crosslinking. The phase separation of rubber within the matrix toughens the glassy matrix because the dispersion induces shear yielding of the matrix and subsequent crack-tip blunting.[3,4]

The majority of published studies on toughened thermosets are based on various types of synthetic liquid rubbers, such as carboxyl-terminated butadiene acrylonitrile (CTBN) copolymer,[5–9] hydroxyl-terminated polybutadiene (HTPB),[10] vinyl-terminated butadiene-acrylonitrile,[11,12] amine-terminated butadiene acrylonitrile (ATBN),[13] styrene-butadiene, and acrylonitrile-butadiene (NBR).[14] However, there are not many reports on liquid natural rubber (LNR).

LNR is depolymerized natural rubber (NR). LNR consists of shorter polymeric chains and has molecular weights ($\overline{M_w}$) lower than 10^5 (g/mol). Material scientists have been interested in

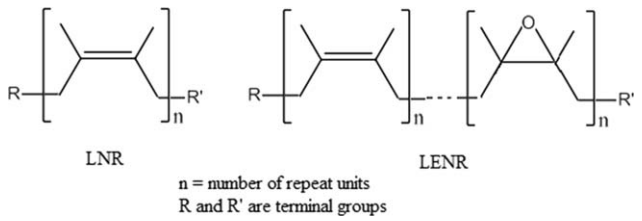

Scheme 1. Chemical structure of LNR.

preparing LNR, because of its strong adhesive power, excellent crosslinking reactivity, and excellent renewability. LNR consists of isoprene units, which is the basic structure of NR.

Epoxidized natural rubber (ENR) is a derivative from the chemical modification of NR, which is derived from the partial epoxidation of the NR molecule, resulting in a new type of elastomer. With a part of C═C double bonds on the NR molecular chains being converted into the polar epoxy groups to obtain ENR, the free volumes of chain phases are decreased and the density and polarity of the derivative is increased. The main difference between NR, LNR and ENR, LENR is the presence of terminal reactive groups in liquid rubbers. Scheme 1 illustrates the structure of LNR and LENR.

Most of the methods for the preparation of LNR are based on using NR latex.[15] However, until date, there are not many reports on the preparation of LNR and liquid epoxidized natural rubber (LENR) using dried NR and ENR. Our laboratory is interested in preparing LNR and LENR from dried NR according to the method mentioned in a patent by Abdullah.[16] The method is based on the sensitized degradation of rubber by visible light. Obtained liquid rubber contains functional groups such as —OH, —OOH, and C═O[17] as a result of oxidation. These groups act as active centers in the liquid rubber polyisoprene chain.

Previous studies showed persistence research of scientists in generating LNR acceptable in the industry, but unfortunately almost all methods involve toxic chemical reagents harmful to the environment. The method used to produce LNR in this research, has some advantages to be commercially acceptable. For example, the reagent used did not have an adverse effect on rubber or polyisoprene chains, the catalyst used will not be interrupted by nonrubber components, the process is efficient and economic, the reagents are noncarcinogenic or toxic to the operator and the process does not leave a residue that could act to disrupt the final products.

Table I. The Range of Molecular Weight of Resin and Rubbers

Sample	M_w (g/mol)
UPR	2×10^3–3×10^3
NR	2×10^6–9×10^6
ENR	2×10^6–3×10^6
LNR	3×10^5–6×10^5
LENR	2×10^5–4×10^5

LNR can be used as a raw material to improve processibility of the rubbers used in viscosity modifiers, adhesives, pressure-sensitive adhesives, sealing agents, caulking compounds, and plasticizers. LNR can also be used as a compatibilizer in thermoplastic NR.[18,19] For instance, LNR has been used as compatibilizer in a polypropylene/NR blend,[20] and was found to increase the adhesion between PP and NR owing to the presence of active groups along the polyisoprene chains. In a study on high-density polyethylene/NR (HDPE/NR-40/60) blend with LNR as the plasticizer, it was observed that a gradual increase in LNR content increased the tensile strength and elongation at break.[21] Liquid rubber can be easily modified chemically because of its low molecular weight. The presence of a reactive group and double bond in LNR offers many possibilities for chemical transformations. Compared to dried rubber, the use of liquid rubber is advantageous for the production of various products because it can be processed easily and requires less energy.[22] Moreover, LNRs have two major advantages over the synthetic rubbers mentioned above. First, the synthetic route for the preparation of LNR and LENR is more green and more energy efficient than other technologies such as metathesis degradation and cleavage by periodic acid and lead tetra acetate.[23–25] In addition, NR can be obtained from natural resources (green route).

The present study evaluates and compares the use of LNRand LENR as an impact modifier for UPR. We also investigate the effects of both liquid rubbers on the thermal and morphological properties of UPR.

EXPERIMENTAL

Materials

The materials used in this study were standard Malaysian rubber-latex (SMR-L) grade NR (NR) and epoxidized NR (ENR-50) purchased from the Malaysian Rubber Board. SMR-L is abbreviation of Standard Malaysian Rubber-Latex, with the plasticity retention index of 60 and Wallace rapid plasticity (P_o) of 35. The UPR used was an orthophthalic UPR containing 30% styrene supplied by Revertex (M) Sdn. Bhd. Methyl ethyl ketone peroxide was used as the initiator. Other components such as methylene blue, toluene, rose Bengal, and methanol were purchased from Sigma-Aldrich. LNR and LENR were generated in our laboratory by photosensitized degradation of NR and ENR, respectively.[17,26]

Dried NR (1 kg of NR or ENR) was cut into small pieces and soaked in toluene overnight followed by the addition of a mixture of methylene blue (0.10 g) and rose Bengal (0.15 g) in methanol. The solution was stirred frequently using a mechanical stirrer in the presence of visible light (fluorescent lamp, 40 watt) with the storage temperature of 80°C, for almost 2 weeks until the rubber mixture transformed into a golden-yellow viscous liquid. Good-quality LNR usually has a yellowish appearance and honey-like viscosity.[17,26] Purification of LNR and LENR was carried out by centrifugation for 4 min at 3000 rpm. This process removed and separated the NR or ENR gel, which floats on the surface of the tube, from the liquid rubber. The molecular weights (M_w) of the ensuing LNRs were measured by gel permeation chromatography (GPC), Model PL- GPC 50 plus. The range of molecular weight

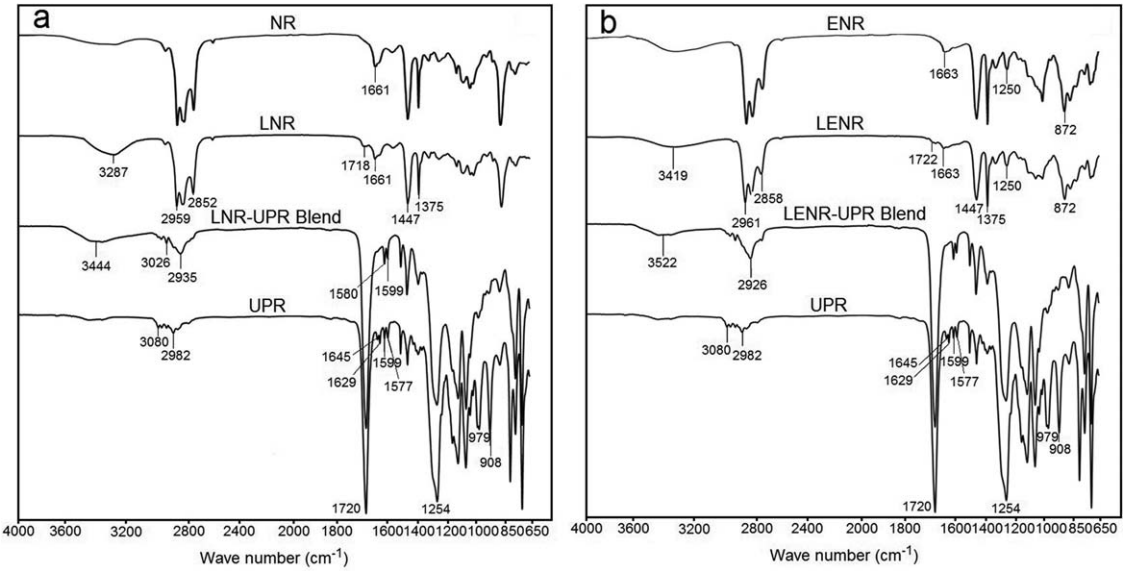

Figure 1. ATR-FTIR spectra of: (a) NR, LNR, UPR, and the LNR-UPR blend; (b) ENR, LENR, UPR, and the LENR-UPR blend.

of resin and both rubbers, before and after photochemical degradation, are listed in Table I.

Preparation of UPR–Liquid Rubber Blends

Different amounts (1.5–6.0 wt %) of LNR or LENR were added to the polyester resin and mixed using a mechanical stirrer for approximately 3 h, followed by the addition of the initiator (1.5 wt %). The mixture was stirred for a further 2 min, poured into the mold, and cured at room temperature for 24 h.

Analysis and Testing

Infrared Spectroscopy. Attenuated total reflectance-Fourier transform infrared (ATR-FTIR) spectroscopy (Perkin Elmer) was used to examine any change in the functional groups that may have been induced by the crosslinking process. The samples were analyzed in transmittance mode within the range 4000–600 cm^{-1}.

Morphology Analysis. The fracture surface of neat and modified resins after impact test, were investigated using field emission scanning electron microscopy (FESEM, Zeiss Supra 55VP model). The samples were sputter-coated with gold to avoid charging. Image analyzer was used to measure the dimensions of the rubber particles.

Optical three-dimensional (3D) surface metrology was performed using an Alicona Infinite Focus Microscope (IFM) at 10 × Magnification. For these experiments, the rubber phase was preferentially extracted using toluene for 24 h at room temperature and then dried in the oven overnight.

The number- (D_n), weight- (D_w), volume- (D_v), and area-average diameter (D_a), polydispersity index (PDI), volume fraction of dispersed phase (Φ) per unit volume, and the interfacial area per unit volume were calculated from the following equations.[27]

$$\overline{D_n} = \frac{\sum n_i D_i}{\sum n_i} \quad (1)$$

$$\overline{D_v} = \frac{\sum n_i D_i^4}{\sum n_i^3} \quad (2)$$

$$\overline{D_w} = \frac{\sum n_i D_i^2}{\sum n_i D_i} \quad (3)$$

$$\overline{D_a} = \left(\sum n_i D_i^2 / \sum n_i\right)^{1/2} \quad (4)$$

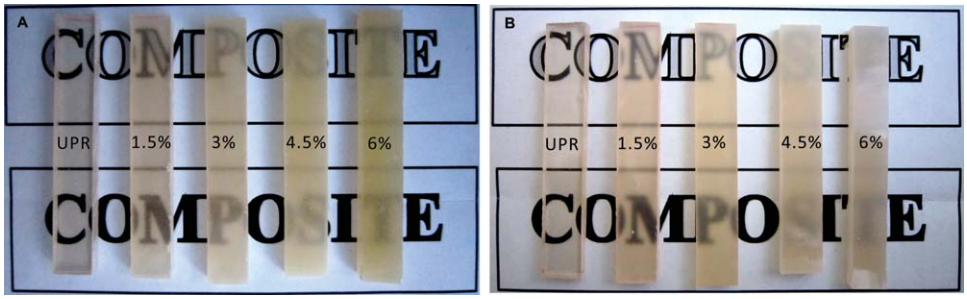

Figure 2. Photograph of neat and modified UPRs (a) LNR-UPR and (b) LENR-UPR. [Color figure can be viewed in the online issue, which is available at wileyonlinelibrary.com.]

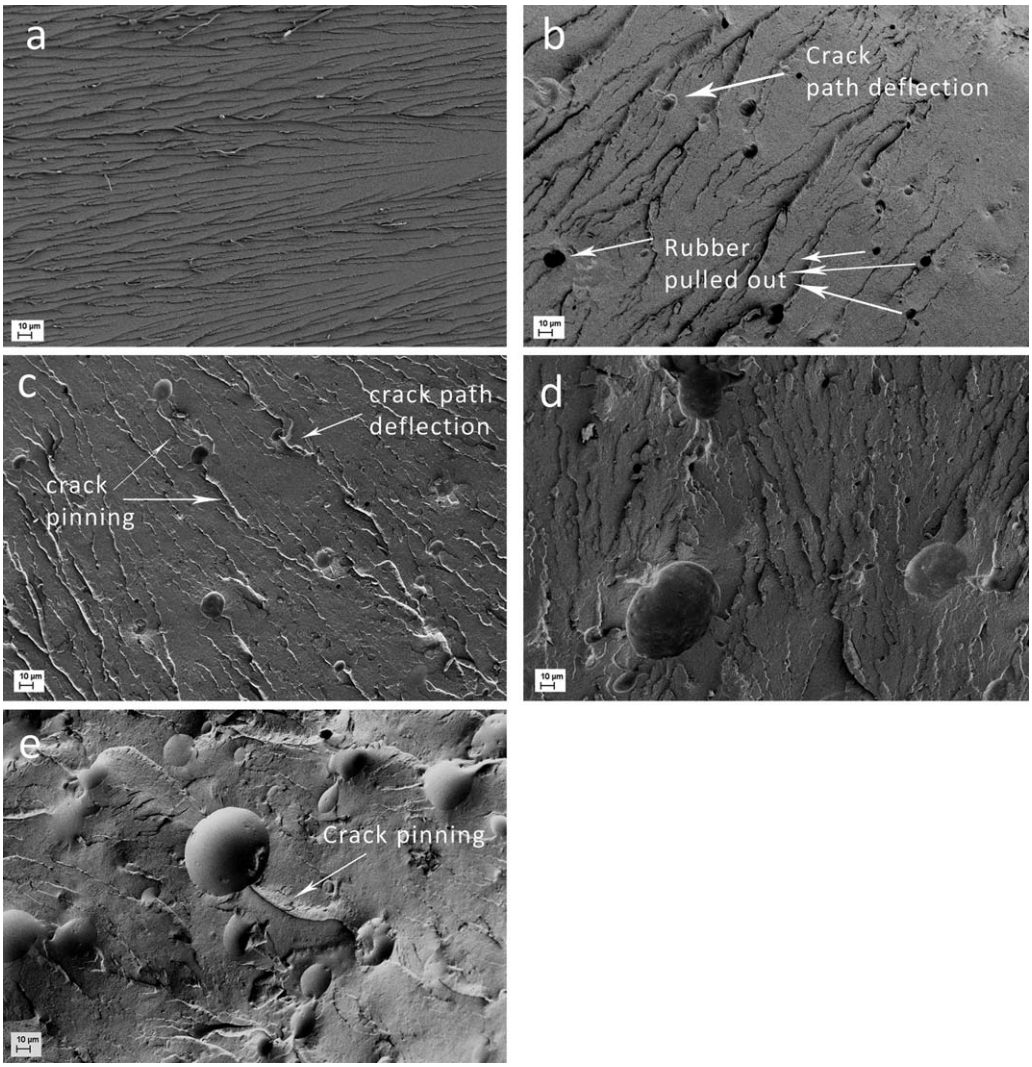

Figure 3. FESEM images of the fractured surface. (a) Neat UPR and (b–e) LNR-based blends with 1.5, 3, 4.5, and 6 wt % of LNR, respectively.

$$\mathrm{PDI}=\frac{\overline{D_w}}{\overline{D_n}} \tag{5}$$

$$\Phi=\frac{\pi}{4}\left(\frac{\sum nD^2}{A_{\mathrm{ref}}}\right) \tag{6}$$

$$\text{Interfacial area per unit volume}=\frac{3\Phi}{r} \tag{7}$$

where A_{ref} is the area of micrograph region under analysis, D is the diameter of domains, r is the radius of the domains, and Φ is the volume fraction of the dispersed phase per unit volume.

Mechanical Measurements. Tensile testing of specimens was carried out using an Instron Universal Testing Machine (model 5567) with a crosshead speed of 5 mm/min according to ASTM D-638-91 Standard Test Methods for tensile properties of unsaturated polyester. The specimens were cut to dimensions of 160 × 13 × 3 mm^3 from cured sheets. These values were the average of 10 specimens.

The impact strength of un-notched specimens was measured according to ASTM D4812 Impact Resistance of Plastic. Tests were run on a RAY-RAN digital Universal pendulum impact tester at room temperature, and the results were averaged over eight samples.

The fracture toughness was measured in terms of critical stress intensity, K_{IC}. Fracture toughness values have been determined using single-edge-notched specimens in three-point bending with a span of 40 mm. The test were performed at room temperature (25°C) in Charpy mode using an Instron Dynatup 9210 Falling Weight Impact Tester with a V-shaped impactor tip and a crosshead speed of 5 m/s. The length, breadth, thickness, and notch length of the specimens were 60, 10, 3, and 2 mm, respectively. K_{IC} was determined according to ASTM D5054-99 using the following relationship:

$$K_{\mathrm{IC}}=\frac{F_{\max}}{BW}a^{1/2}f\left(\frac{a}{W}\right) \tag{8}$$

where $F_{\max}$ is the maximum force from the load-elongation trace, B is the thickness of the specimen, W is the width of the

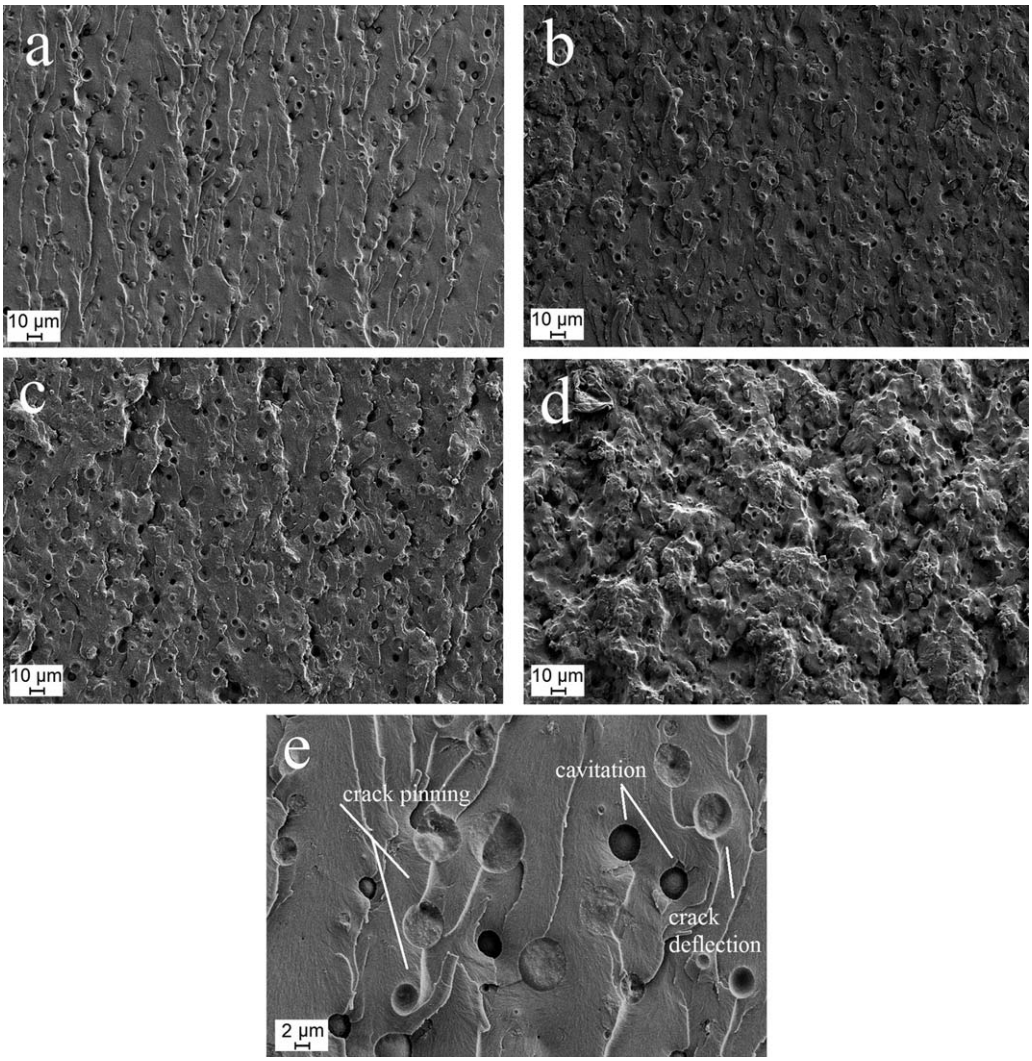

Figure 4. FESEM images of the fractured surface of LENR-based blends with (a) 1.5 wt %, (b) 3 wt %, (c) 4.5 wt %, and (d) 6 wt % LENR; (e) blend with 1.5 wt % LENR (at higher magnification).

specimen, and a is the total notch length. $f\left(\frac{a}{W}\right)$ is the corresponding geometry correction factor and is expressed as described previously[28]:

$$f\left(\frac{a}{W}\right)=1.93-3.07\left(\frac{a}{W}\right)+14.53\left(\frac{a}{W}\right)^2-25.11\left(\frac{a}{W}\right)^3+25.80\left(\frac{a}{W}\right)^4 \quad (9)$$

Critical strain energy release rate (fracture energy) G_{IC} was computed using the expression,

$$G_{IC}=\left(\frac{K_{IC}^2}{E}\right) \quad (10)$$

where E is the elastic modulus.

A dynamic mechanical thermal analyzer (Q800 DMTA, TA instruments) was used to measure the loss of rigidity at high temperatures for neat and all rubber-modified UPRs according to ASTD4065. The temperature dependence of the storage modulus (E'), loss modulus (E''), and the loss factor (tan δ) were studied. Measurements were carried out from −100 to 150°C at a heating rate of 5°C min^{-1}, with a fixed frequency of 1 Hz. Single cantilever mode was used for the sample of size 35 × 13 × 3 mm^3.

Thermogravimetric Analysis. Thermogravimetric analysis (TGA) was performed with a Mettler Toledo SDTA 851e thermal analyzer to investigate the thermal stability of the cured samples of both neat and rubber-modified UPR. About 10 mg of sample was heated in a platinum crucible from room temperature to 600°C at a heating rate of 10°C/min under a nitrogen atmosphere.

RESULTS AND DISCUSSIONS

Infrared Spectroscopy

ATR-IR spectroscopy was used to analyze the occurrence of any chemical interactions between UPR and LNR or LENR. The ATR spectra of the neat components and rubber-modified blends are shown in Figure 1. The spectrum of neat UPR shows a strong signal at 1720 cm^{-1} and two signals at 1599 and 1577 cm^{-1}. These can be assigned to the C═O stretch of

Table II. Range of Rubber Particle Size in UPR Matrix

	Diameter (μm)	
Rubber solid content (%)	LNR	LENR
1.5	6–25	1–5
3	8–40	1–7
4.5	8–50	1–7
6	12–65	1–5

carboxylic acids and the C═C stretch absorption of the ring skeleton in styrene and UPR, respectively. The signals at 908 and 1629 cm^{-1} are attributed to C═C stretching in styrene. Other signals at 979 and 1645 cm^{-1} are attributed to C═C stretching of the UPR chains (Figure 1).

Figure 1(a) shows the ATR spectra of NR and LNR. On comparing the spectra for LNR and NR, we observe some apparent changes in the LNR spectrum around 3200−3500 and 1718 cm^{-1}. These were assigned to the OH stretching of OOH and alcohol groups and the C═O stretching, respectively. These two prominent signals are characteristic of the oxidation products formed from the photochemical degradation of the polyisoprene chain.[17]

The FTIR spectrum of LENR is similar to the spectrum of ENR and shows two signals attributable to the epoxy ring at 1250 and 872 cm^{-1}. The broad signal around 3400 cm^{-1} is due to the OH stretching. The signal at 1663 cm^{-1} is assigned to C═C stretching in rubber. Two other strong signals at 1447 and 1375 cm^{-1} are attributed to the —CH_3 and —CH_2 absorption, respectively. Interestingly, the spectrum of LENR also shows a signal at 1722 cm^{-1}, that could be assigned to a C═O stretch, which formed after the photochemical degradation of ENR[29] [Figure 1(b)].

Several of these signals change as a result of chemical interactions within the blend. It can be clearly observed from Figure 1(a,b) that the consumption of the styrene monomer in the cured blends caused the signals at 908 and 1629 cm^{-1} to disappear, whereas the consumption of the C═C bond in the unsaturated polyesters caused the signals at 1645 and 979 cm^{-1} to disappear. The disappearance of these signals from the spectrum for both the blends, indicated full participation of the functional groups (C═C) in crosslinking. The signals observed in

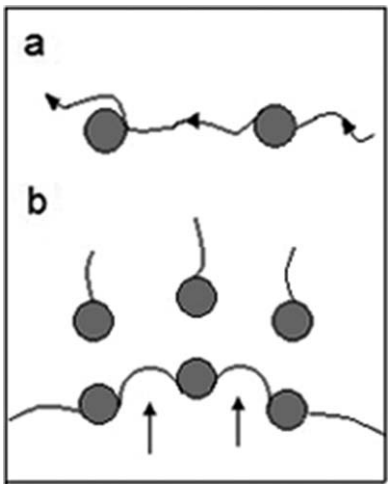

Figure 5. Schematic illustrating the (a) crack deflection and (b) crack-pinning mechanisms. The spherical shapes denote elastomeric particles. The lines and arrows represent crack propagation energy and energy, respectively.

the spectra for both the blends in the range 2800−3100 cm^{-1} is related to the CH stretching of CH_2 and CH_3. These signals became sharper compared to the signals observed in neat UPR. However, the intensity of these signals was lower than the signal intensities observed for the rubber-modified UPRs [Figure 1(a,b)]. This result is indicative of the crosslinking process as all the C═C bonds were converted to C—C bonds. Furthermore, the increment in the intensity of the two signals (attributable to the —CH bending) at 1452 and 1378 cm^{-1} in the spectrum of both the blends is further evidence for the crosslinking.

The spectrum of the LENR-UPR blend shows that the absorption band corresponding to the epoxy ring at 872 cm^{-1} disappeared after the crosslinking. This observation indicates that in addition to the physical interaction between UPR and the terminal active groups, the epoxy ring contributed to the crosslinking by chemically bonding with C═C of UPR. However, no evidence of a similar chemical interaction was found in the spectrum of LNR-UPR. We believe that LNR, unlike LENR, possibly only interacted physically with UPR via its terminal active groups. However, in the case of LENR, epoxy group has potential to have chemical interaction with C═C of UPR Morphological observations in the following section support this statement.

Table III. Number-, Area-, Weight-, and Volume-Average Diameter of Domains Dispersed in the Polyester Matrix

Rubber content	$\overline{D_n}^a$ (μm)	$\overline{D_a}^b$ (μm)	$\overline{D_v}^c$ (μm)	$\overline{D_w}^d$ (μm)	PDI	Φ	$^{3\Phi}/_{r}$
1.5% LNR	16.0	17.7	4.9	19.5	1.18	12.4	3.6
3.0% LNR	16.6	18.1	5.0	19.8	1.19	19.3	5
4.5% LNR	17.3	19.8	9.7	22.6	1.30	30.3	6.9
6.0% LNR	26.4	30.4	37.9	35.1	1.32	33.8	7
1.5% LENR	2.75	2.88	0.045	2.87	1.04	26.27	51.5
3.0% LENR	2.86	3.08	0.063	3.33	1.16	41.20	73.2
4.5% LENR	3.32	3.61	0.078	3.93	1.18	49.95	99.9
6.0% LENR	3.35	3.88	0.080	3.95	1.17	97.65	177

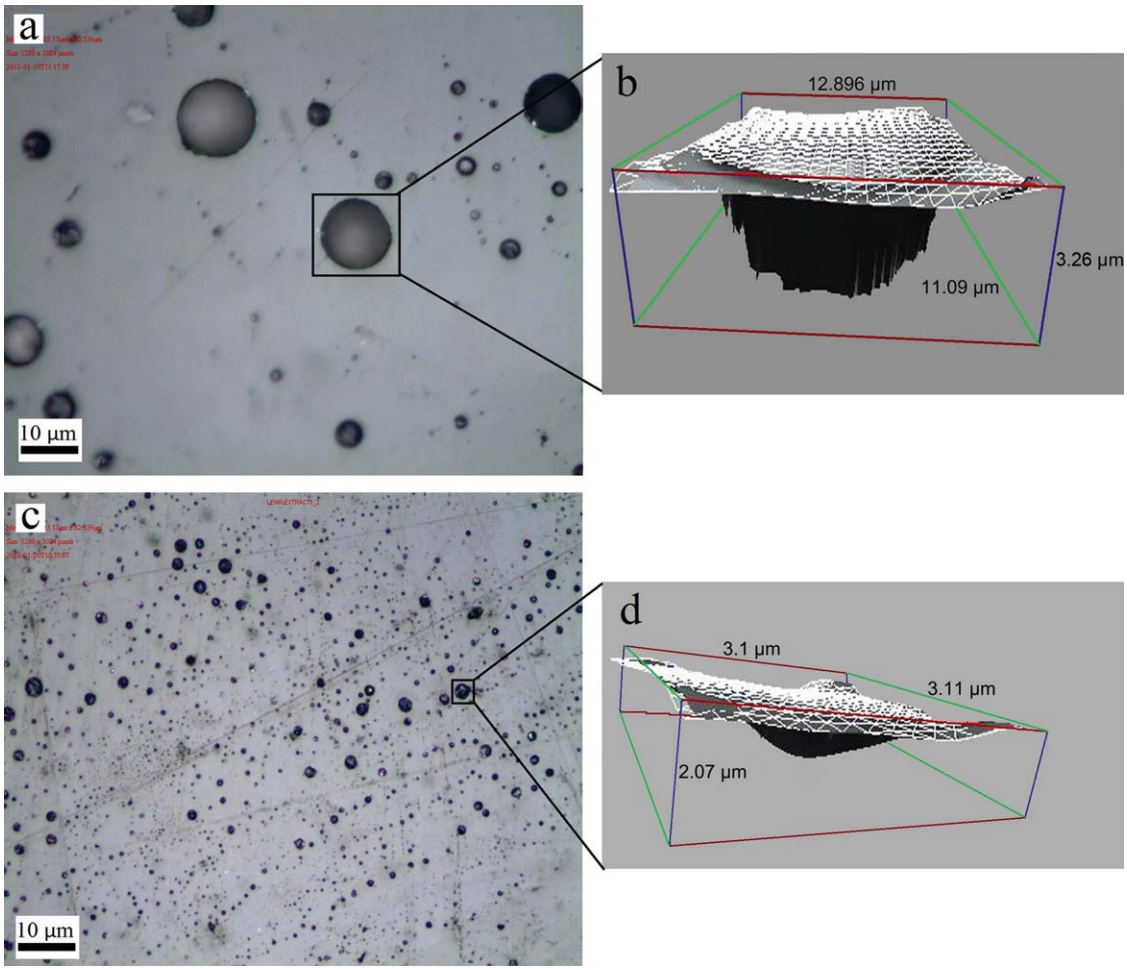

Figure 6. Optical 2D and 3D images of the rubber-modified UPRs. (a, c) 2D images of 1.5 wt % LNR- and LENR-modified UPR, respectively. (b, d) 3D images of 1.5 wt % LNR- and LENR-modified UPR, respectively. [Color figure can be viewed in the online issue, which is available at wileyonlinelibrary.com.]

Morphology of Rubber-Modified Unsaturated Polyester

Figure 2 shows the appearance of the various samples. It can be seen that while the neat UPR was transparent, the opacity of the material increased with the LNR or LENR content. This loss in the transparency is suggestive of the heterogeneous morphology of the blends.

The fractured surface of the neat and rubber-modified UPR samples was examined using FESEM (Figures 3 and 4). The fractured surface of all the modified UPR samples clearly showed two distinct phases: a continuous matrix and a dispersed rubber phase. This result was also in accordance with the visual inspection of the blends. The neat UPR sample [Figure 3(a)] displayed a smooth and glassy fractured surface with ripples. The ripples are due to the brittle fracture of the network, which accounts for its poor impact strength as there is no energy dissipation mechanism operating in this case.[8] However, the fractured surfaces of all the modified UPR samples, unlike neat UPR, were rougher, indicative of ductile fracture.

It can be seen in Figures 3 and 4 that the size of the precipitated rubber domains in the LENR-modified resin is smaller than the size of the rubber domains in the LNR-UPR blends. The rubber domains in the LNR blend exhibited a broad size distribution from 6 to 64 μm, whereas the size of the rubber domains for the LENR-modified resin was in the range of 1 to 7 μm (Table II). Moreover, it was observed that the size of the precipitated rubber domains in LNR-UPR increased with the elastomer content, probably due to coalescence of the rubber particles (Figure 3). In contrast, LENR showed prodigious behavior with no increase in the size of rubber particles with increasing rubber content up to 4.5 wt % (Figure 3). On increasing the LENR content in the blend up to 6 wt %, we observed a decrease in the particle size. This may due to the higher compatibility and miscibility of LENR as a result of the chemical interactions with the UPR matrix. At 6 wt %, some LENR may dissolve in the matrix instead of forming phase-separated particles.

The average diameter and distribution of the precipitated rubber domains along with other related data are listed in Table III. The results agree well with the qualitative microscopic observations, that is, higher number- and area-average domain diameters for

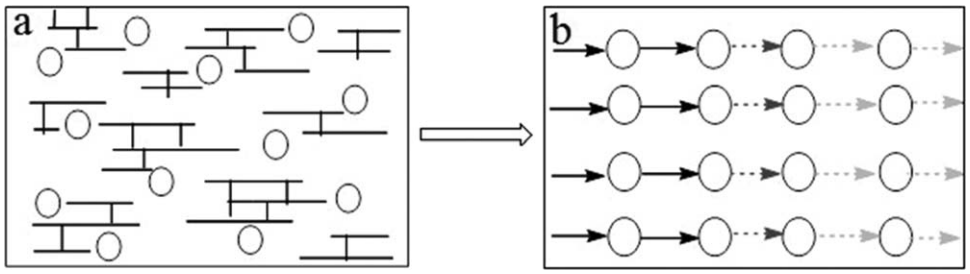

Scheme 2. Schematic illustrating the crosslinked network and energy transfer through the rubber particles in the LENR-UPR system. The spherical shapes denote elastomeric particles adhered to the UPR matrix. The arrows represent the crack propagation energy. The energy dissipation is represented by the decrease in the size and transparency of the solid arrow.

LNR-based blends. The values of the number- and area-average domain diameters increased continuously with the rubber content for LNR-based blends. The results obtained for LNR-modified UPR agrees with data reported in the literature for other rubber-modified thermosets.[8] The increase in the domain size of the LNR phase is associated with coalescence of the dispersed rubber particles. This phenomenon was more prominent at higher concentrations of the LNR phase. In stark contrast, increasing the rubber content did not induce any significant change in the domain size of the LENR phase. The PDI of the rubber domain size was significantly higher for LNR-based blends compared to that for LENR-based blends (Table III).

The compatibility and interaction of rubber with the UPR matrix can be determined by computing the volume fraction (Φ) and interfacial area of the dispersed rubbery phase. The interaction of the rubber domains with the UPR matrix increases with the interfacial area.[5] The interfacial area per unit volume between the dispersed and continuous phases was much higher for LENR-modified UPR compared to that for LNR-based blends. This was a consequence of the smaller particle size of the dispersed phase in LENR-modified UPR (Table III). This was also further proof for stronger interactions present between LENR and UPR when compared to interactions present between LNR and UPR.

The fracture mechanism can also be explained via morphological investigation. The main fracture mechanisms observed in both the modified polyesters were particle cavitation, shear yielding, crack pinning, and crack path deflection. In addition, both LNR and LENR-modified polyesters exhibited a stress-whitened zone on the fracture surface. This zone formed during the loading sequence, and its size was proportional to the increase in toughness. Therefore, examining the size of this zone was necessary for the elucidation of the toughening mechanism.[30] Stress whitening is due to the scattering of visible light from the voids (scattering center) formed in the matrix as a result of the cavitation of rubber particles.[31] Compared to the LNR-modified polyester, the LENR-modified polyester showed a wider stress-whitened zone indicating greater cavitation of the rubber particles. Thus, the LNR-modified polyester exhibited higher toughness (Figures 3 and 4).

It is well known that a homogenous distribution of small particles induced yielding of the matrix. In fact, uniformly distributed rubber particles act as stress concentrators, and therefore, rubber-modified UPRs exhibit higher impact strength than unmodified UPR.

The micrographs of LENR-UPR displayed a homogenous dispersion of smaller rubber particles even at high rubber content [Figure 4(a–d)]. In contrast, the micrograph of LNR-UPR [Figure 3(b)] showed uniformly distributed small and spherical elastomer particles only with 1.5 wt % of LNR, whereas an inhomogeneous distribution of phase-separated rubber domains was observed at higher weight content of LNR [Figure 3(c–e)]. Therefore, higher impact properties were expected for the LENR-UPR blend.

Crack pinning, another toughening mechanism, was the more dominant mechanism in both the modified polyester systems. According to this mechanism, the proposed role of the rubber particles is to behave as impenetrable objects that cause the crack to bow out. This consumes extra energy. The difference in the toughness between the brittle polyester and the ductile rubber phase is large enough for these particles to be considered relatively impenetrable. Indirect evidence for the crack pinning mechanism comes from the occurrence "tails" near the particles on the fracture surface[32] (Figure 5).

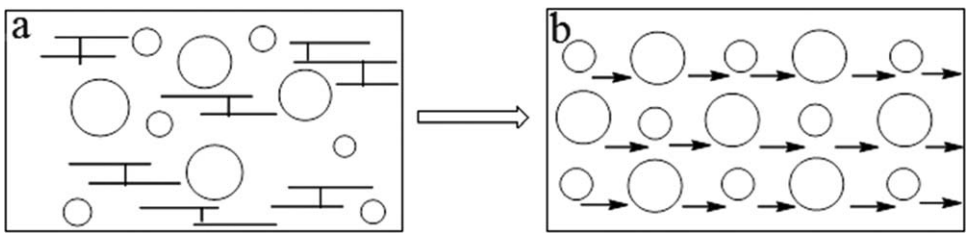

Scheme 3. Schematic illustrating the crosslinked network and energy transfer through the rubber particles in the LNR-UPR system. The spherical shapes denote elastomeric particles adhered to the UPR matrix. The arrows represent the crack propagation energy. The energy dissipation is represented by the decrease in the size and transparency of the solid arrow.

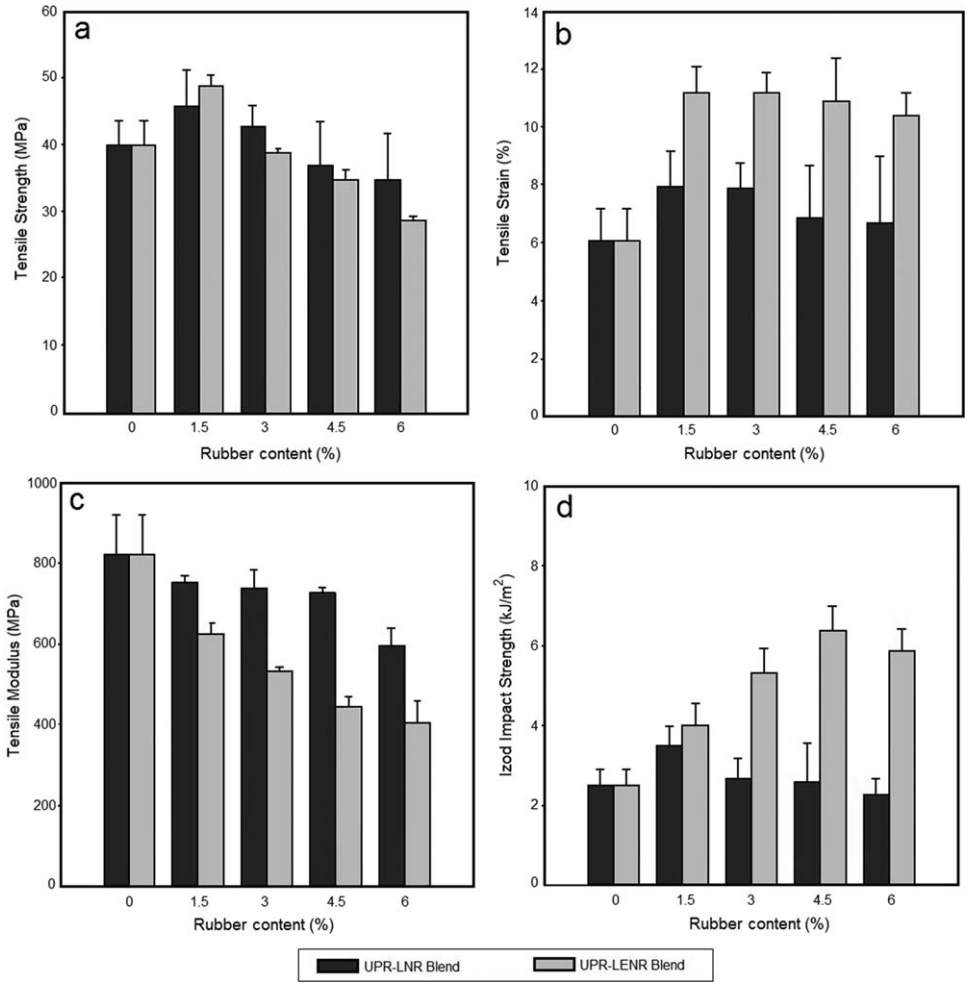

Figure 7. Tensile and impact properties of UPR-LNR and UPR-LENR blends. (a) Tensile strength, (b) Tensile strain, (c) Tensile modulus, and (d) Izod impact strength.

According to the crack-path deflection mechanism, the proposed role of the rubber particles is to cause the crack to deviate from its main plane resulting in increased surface area. It would also reduce the opening of the crack on both sides, thereby increasing the energy required to propagate such a crack. Figure 5 shows a schematic illustrating of crack pinning and crack path deflection mechanisms.

Table IV. Tensile and Impact Properties of Neat UPR, LNR-UPR, and LENR-UPR Blends

Sample	Tensile strength (MPa)	Tensile strain (%)	Modulus (MPa)	Impact energy (kJ/m^2)
UPR	40 ± 3.4[a]	6.1 ± 1.1	821 ± 50	2.5 ± 0.4
1.5% LNR	46 ± 5.2	7.9 ± 1.2	752 ± 16	3.5 ± 0.5
3.0% LNR	43 ± 2.9	7.9 ± 0.9	738 ± 45	2.7 ± 0.5
4.5% LNR	37 ± 6.5	6.9 ± 1.8	727 ± 14	2.6 ± 1.0
6.0% LNR	35 ± 6.7	6.7 ± 2.3	596 ± 45	2.3 ± 0.4
1.5% LENR	49 ± 1.5	11.2 ± 0.9	624 ± 28	4.0 ± 0.5
3.0% LENR	39 ± 0.5	11.2 ± 0.7	531 ± 12	5.4 ± 0.6
4.5% LENR	35 ± 1.5	10.9 ± 1.5	445 ± 24	6.4 ± 0.6
6.0% LENR	29 ± 0.5	10.5 ± 0.8	403 ± 40	5.9 ± 0.5

[a] The values in the table are mentioned as mean ± s.d.

The FESEM micrographs of LENR-modified polyester show that the rubber particles were partly fractured and that less rubber was pulled out [Figure 4(e)]. It indicates that the crack developed through the rubber particles as a result of the interaction between the particle and the matrix. Thus, these samples showed high impact properties. In contrast, the micrographs of the LNR-modified polyester [Figure 3(b)] show that the rubber particles were pulled out from the matrix instead of being fractured. This indicates that energy dissipation occurred through the matrix resulting from the poor interaction between the particles and the matrix.

Optical two dimensional (2D) and 3D surface images of modified polyester systems with 1.5 wt % LNR and LENR rubber are shown in Figure 6. The 2D images are similar in appearance, except for the smooth matrix surface, to the images obtained using FESEM. The empty spaces left behind by rubber particles removed by toluene leaching appear as the dark face in the 3D

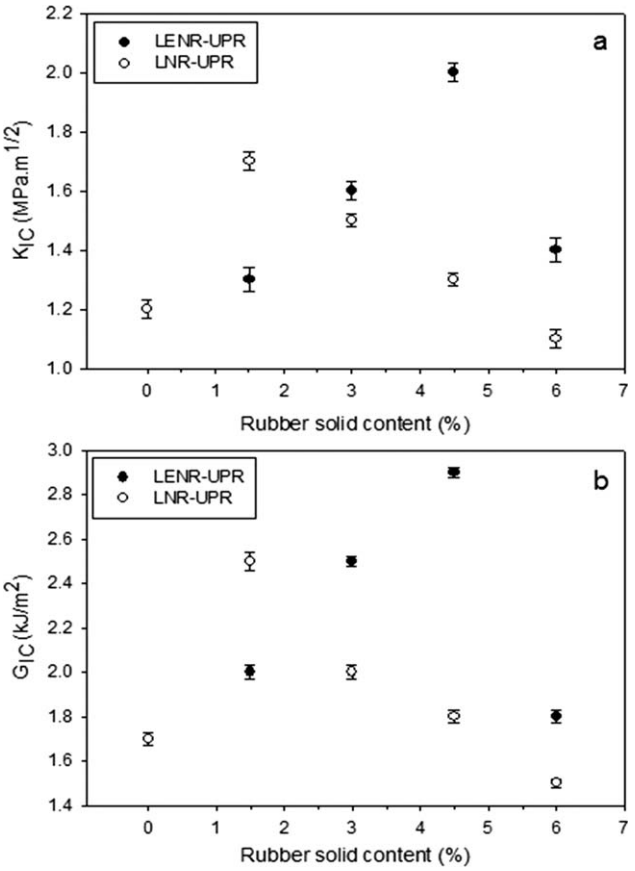

Figure 8. (a) Fracture toughness and (b) fracture energy as a function of rubber content.

images [Figure 6(b,d)]. It can be seen from Figure 6(b) that almost 75% of the rubber was removed in the case of LNR-UPR. In contrast, only 33% of rubber was removed after toluene leaching in the case of LENR-UPR, leaving more rubber remaining in the hole. This could be further evidence for the higher compatibility and interfacial adhesion in LENR-UPR.

Mechanical Properties

Tensile Properties. The tensile properties of LNR and LENR-modified blends are shown in Figure 7 (panels a, b and c), and the corresponding data are listed in Table IV.

The tensile strength for LNR and LENR-toughened UPR is shown in Figure 7(a). The tensile strength of both the systems increased on inclusion of 1.5 wt % of rubber but decreased with the incorporation of more elastomer. This could be due to the better interaction, adhesion, and compatibility of the elastomer with the resin matrix, which is manifested in Figure 7(b,d). The rubber phase was actually formed with microvoids due to resin shrinkage during the curing process. Therefore, the small size of rubber particles resulted in a smaller cracking zone. Moreover, the finer dispersion of the rubber phase in the matrix resin, caused by lower interfacial energy between the components, was attributed to a good adhesion at phase boundaries for 1.5 wt % rubber content. This also improved the stress transfer within the materials.

It is widely accepted that rubber particle size, surface area of contact, the intrinsic strength of the rubber phase, and its compatibility with the thermoset matrix, affect the tensile properties of rubber-toughened resins.[13] Thus, LENR particles with a smaller size and more contact surface area compared to LNR particles at the optimal percentage [Figures 3(b) and 4(a)] displayed higher tensile strength.

Conversely, above the optimum rubber content, the natural fact of increasing of rubber content becomes dominant [Figure 3(c–e)]. The presence of large particles in the blend led to zones through which cracks could pass through easily, thereby reducing the value of the tensile strength.[33] However, we did not observe much increase in the size of the elastomer domains in LENR-modified systems. The reason for the slight reduction in the tensile strength in LENR-UPR systems is attributed to the flexibilization of the matrix (probably to a lesser extent) along with toughening behavior.

It is also worth noting that most of the previous research on toughening thermosets using synthetic liquid rubber, such as CTBN,[34] ATBN,[13] HTPB,[35] and so forth, had observed a significant reduction in the tensile strength. In contrast, 1.5 wt % of LNR and LENR improved the tensile strength by 15 and 22%, respectively (Table IV).

Figure 7(b) shows that the tensile strain increased with the rubber content for both blend systems. In particular, LENR-UPR displayed a dramatic increase in tensile strain values. The reaction was evidenced from IR spectroscopic analysis and explained by the fact that both rubbers hide the effect of the UPR. Since LENR contains a commendable number of epoxide groups, compared to LNR, which contains a small amount of reactive groups resulting from the photo degradation, it is reasonable to expect that its rubber particles are more compatible with the UPR matrix. Thus, the LENR-UPR system showed excellent tensile strain values (Table IV).

In agreement with many studies,[34,36,37] the tensile modulus of both systems decreased gradually with increasing rubber content [Figure 7(c) and Table IV]. It is attributed to the effect of the soft segment structure of LNR and LENR as well as to the intrinsically low modulus of liquid rubbers compared with neat UPR.[8,38] It is interesting to note that the tensile modulus of LENR-UPR blend showed more reduction in contrast with LNR-UPR blend. The reason was due to the better interaction of LENR and UPR that emphasized the rubbery properties of blend more than LNR-UPR blend. In fact, the better interaction and the resultant tensile properties were caused by the homogeneous distribution of the comparatively smaller particles in LENR-modified blends.

Impact Properties. Figure 7(d) depicts the Izod impact strength of the un-notched neat, LNR-, and LENR-modified UPR. The corresponding values are listed in Table IV. Both the modified blends showed higher impact resistance compared to the neat resin. However, LENR-toughened UPR showed a higher increment in impact strength compared to that shown by LNR-modified UPR. In rubber-modified UPR, the improvement in impact strength can be correlated to the enhancement in the

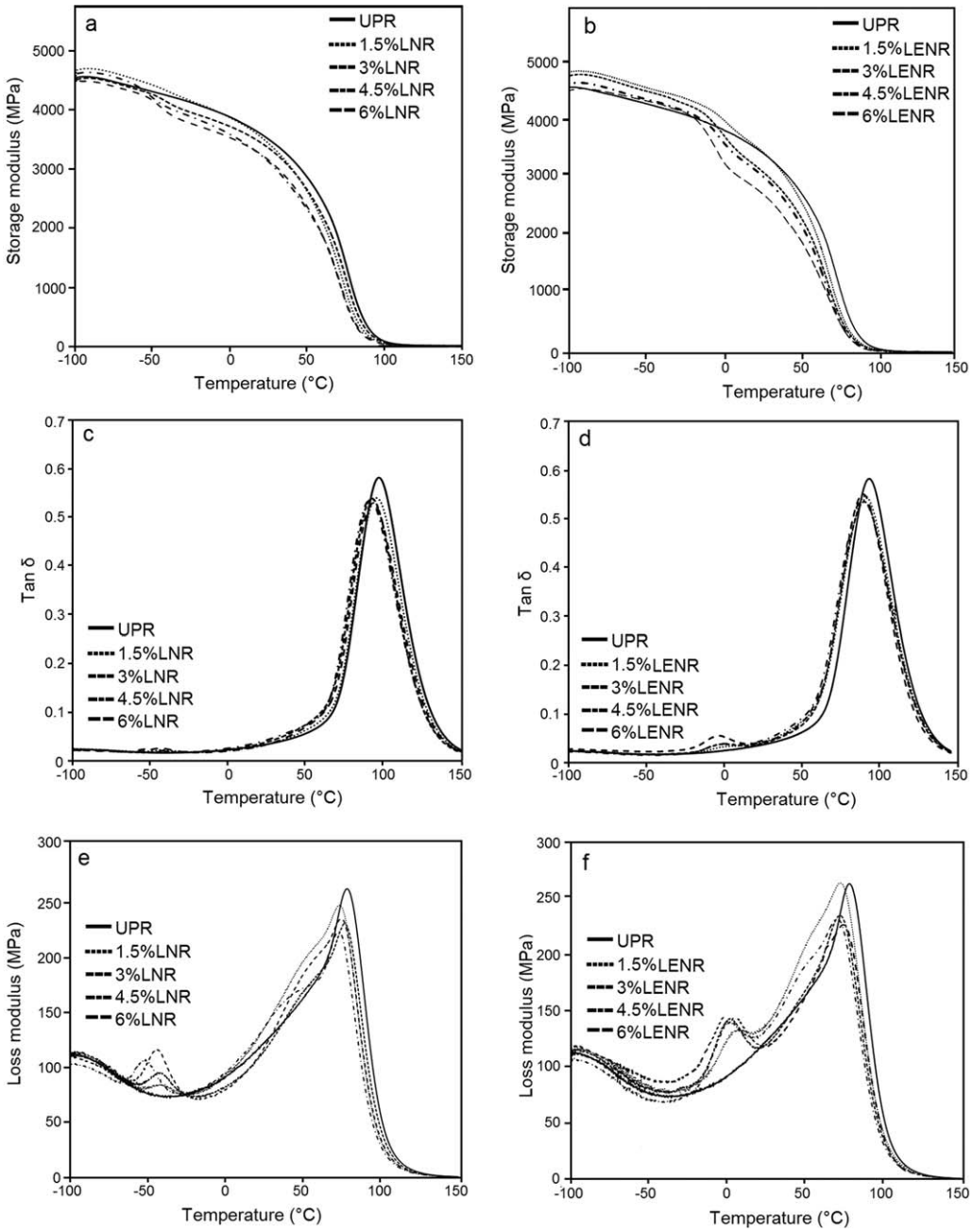

Figure 9. DMA results for LNR-UPR and LENR-UPR. (a, b) Temperature dependence of the storage modulus; (c, d) temperature dependence of the loss factor (tan δ); (e, f): temperature dependence of the loss modulus.

toughness. The LENR-UPR blend, which contains 4.5 wt % rubber, has a maximum impact strength value of 6.36 kJ/m^2, which is about 154% larger than the value obtained for neat UPR (2.5 kJ/m^2). In contrast, the maximum impact strength value of 1.5 wt % rubber LNR-modified UPR shows only a 40% improvement over the impact strength for neat UPR. The epoxidized rubber being more reactive and compatible with the resin matrix resulted in higher rubber inclusion, which enhanced the toughness compared to LNR, which interacted less with the resin matrix. Thomas et al.[39] reported only a 47% improvement in impact strength on using a HTBN-modified epoxy matrix. Ratna[40] reported a 60% improvement for a carboxyl-terminated poly (2-ethyl hexyl acrylate) liquid rubber-modified epoxy system.

As mentioned above, LNR-modified UPR exhibited uniformly distributed rubber particles within the matrix only for 1.5 wt % of rubber [Figure 3(b)], and the highest impact strength for LNR-modified UPR (3.5 kJ/m^2) was observed at the same weight percent of rubber. However, this value is still lower than that for the same percentage of LENR-modified UPR (4 kJ/m^2). This can be attributed to the comparatively bigger size and

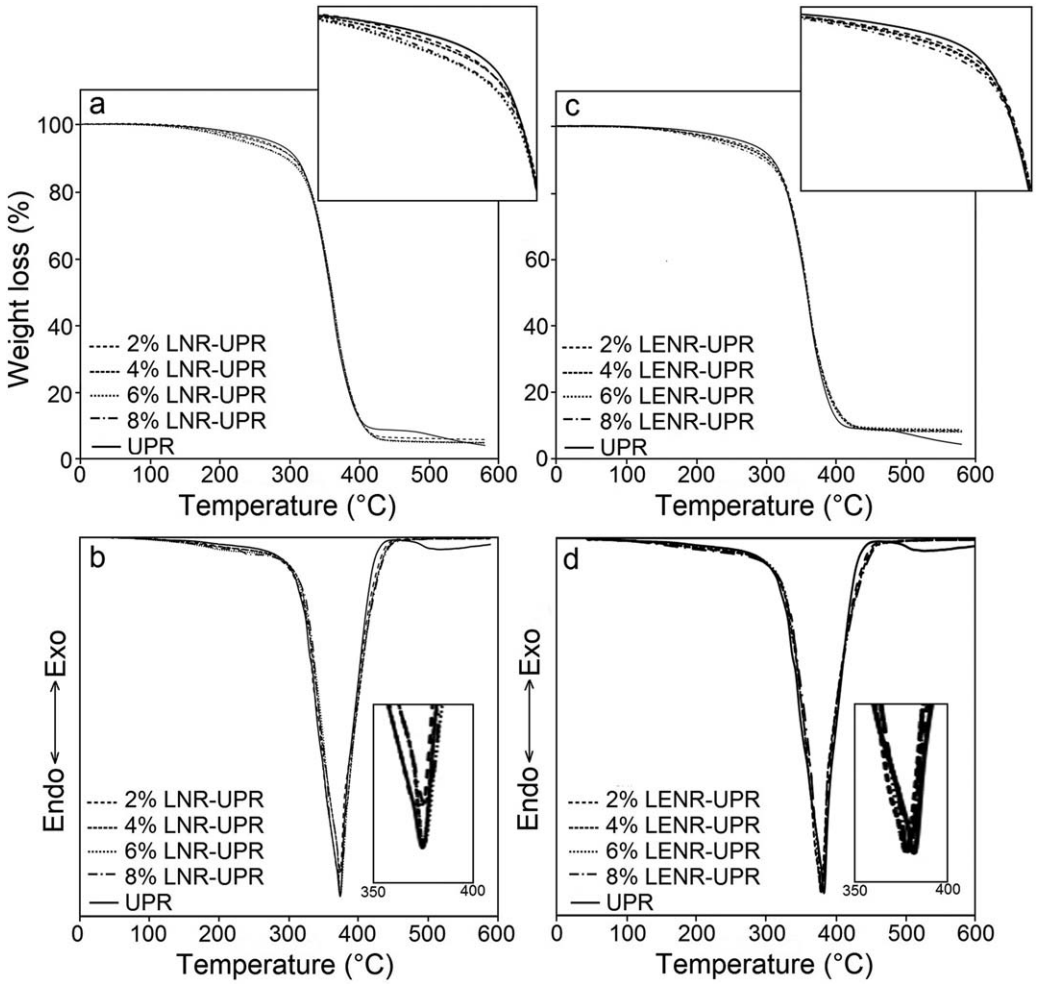

Figure 10. (a) TGA curves for neat UPR and LNR-UPR, (b) DTG curves for neat UPR and LNR-UPR, (c) TGA curves for neat UPR and LENR-UPR, and (d) DTG curves for neat UPR and LENR-UPR. The inset in each figure represents a zoomed in view of the area of interest in each graph.

nonhomogeneous distribution of rubber domains in the LNR-modified matrix compared to the rubber domains in LENR-UPR. The decrease in the impact strength above the optimal LNR content (1.5 wt %) is also ascribed to the lower compatibility of the rubber with the matrix, and the aggregation of rubber particles with increasing rubber concentration. In fact, large elastomeric domains act as deflection sites and lead to catastrophic failure of the matrix. Similar behavior has also been reported for rubber-modified epoxy systems.[33,39,40]

Table V. DMA Values for Neat UPR and LNR/LENR-Modified UPR

Sample	Storage modulus (MPa) at −100°C	T_g (°C)[a]
UPR	4562	94
1.5% LNR	4691	90
3.0% LNR	4528	88
4.5% LNR	4618	88
6.0% LNR	4500	89
1.5% LENR	4819	90
3.0% LENR	4754	90
4.5% LENR	4619	89
6.0% LENR	4450	89

[a] T_g was taken from the main peak of the tan δ versus temperature curves.

Good bonding at the rubber-resin interface along with excellent dispersion of the rubber particles in the UPR matrix is necessary for improving impact resistance. The increase in impact strength up to an optimal rubber concentration is attributed to the effective stress concentration behavior of the phase-separated rubber particles that amplify the plastic deformation of the highly brittle matrix to a certain extent. According to Bucknall,[41] the rubber particles are considered to bridge the crack as it propagates through the material. Thus, the rubber particles are able to prevent the crack from growing to a catastrophic size. Therefore, matrix ductility attained by the incorporation of rubber is the reason for the improvement in the impact strength of the modified blend over that of neat UPR.

The increase in toughness was also due to the amount of elastic energy stored in the rubber particles during stretching. Thus, the deformation of the rubber particles in the matrix seemed to be

responsible for the enhanced stress transfer and the consequent increase in impact resistance. Shear yielding of the matrix was another possible mechanism that could be operating in these systems. According to this mechanism, the principle function of the rubber particles is to produce sufficient triaxial tension in the matrix to increase the local free volume, thereby enabling extensive shear yielding of the matrix. Thus, crack propagation through the rubber particles along with shear yielding was the main toughening mechanism resulting in enhanced impact behavior.[8,42]

To explain the correlation between the morphology and the resultant toughening characteristics, a model has been proposed by Thomas et al.[39] The primary factors that affected the morphological evolution of the cured systems are the dissimilarity in crosslinking density and size of the rubber domains. Scheme 2(a) represents the dispersion of smaller LENR elastomer domains in the midst of a crosslinked thermoset network. The homogeneous distribution of elastomer particles in the modified polyester system is responsible for the enhanced damping nature of the sample. The particles in such systems act as stress concentrators and on application of a force, energy transfer takes place through these particles and dissipate in due course. Thus, the matrix is protected from catastrophic failure. This energy transfer is schematically represented in Scheme 2(b). The spherical shapes denote elastomeric particles adhered to the UPR matrix. The arrows represent the crack propagation energy from the crack initiation site. The crack propagation energy gradually reduces as it passes through the elastomeric particles (dotted arrows). The energy dissipation is represented by the decrease in the size and transparency of the solid arrow.

Scheme 3(a) illustrates the inhomogeneous distribution of elastomer domains having lower interfacial adhesion to the matrix, which is addressed to a modified UPR with higher weight content of LNR elastomer.

Scheme 3(b) represents the energy propagation mechanism in LNR-modified systems. The energy propagation occurs through the interface of the elastomer domains and the polyester matrix. Proper energy dispersion does not take place through the elastomer domains in these samples. Therefore, there is no reduction in the intensity of the crack propagation energy (denoted by the same style of arrows) as it is not propagated through elastomers. This creates interfacial separation, which ultimately leads to the failure of the matrix.[39]

Fracture Properties. Figure 8 illustrates the effect of rubber content on the fracture toughness (K_{IC}) and fracture energy (G_{IC}), for LNR- and LENR-modified UPR. In the case of LNR-UPR, fracture toughness increased by about 41% with 1.5 wt % of rubber. Meanwhile, LENR-UPR showed the maximum fracture toughness (increase of 66%) at 4.5 wt % of rubber. For both the rubber-modified systems, a further increase above the optimal rubber content resulted in the reduction of K_{IC}. A similar trend is also observed in the case of fracture energy, G_{IC}, with a 47 and 70% increment at the optimum LNR and LENR content, respectively.

It seems that the smaller size of the rubber particles and their homogenous dispersion is responsible for the higher fracture toughness of LENR-UPR. In addition, LENR exhibits desirable chemical bonding with UPR, thereby improving toughness as a result of increasing miscibility of the rubber into the UPR matrix. Hence, some rubber dissolves in the UPR matrix and acts as a plasticizer. In contrast, LNR has no appreciable miscibility with the UPR and only a flexibilizing effect operates in LNR-UPR. This phenomenon also could be another reason for the lower K_{IC} value observed with LNR-modified UPR. Nonetheless, both these effects increased the ability of the matrix to deform under shear.[39]

Dynamic Mechanical Thermal Analysis

The evolution of the storage modulus with different contents of LNR and LENR for both neat and modified UPR is depicted in Figure 9(a,b). All samples showed behavior typical of rubber-modified polyester.[40,43] Neat UPR has a storage modulus around 4562 MPa at −100°C and displayed a behavior characteristic of amorphous polymer. At low temperatures, the polymer is in the glassy state, and the modulus remained roughly constant with temperature. At around 50°C, the modulus started to drop sharply. This drop in the modulus corresponds to the main relaxation of the polyester. However, the modified samples displayed a two-step drop in the modulus [Figure 9(a,b)]. The low-temperature modulus drop, whose magnitude increased with the rubber content, is associated with the glass transition temperature (T_g) of the rubber phase. Results showed that the storage modulus for both the rubber-modified systems increased up to 1.5 wt % rubber and reduced with the incorporation of more rubber. The reduction in storage modulus is attributed to the lowering of the crosslinking density and plasticization of the UPR matrix on addition of the liquid rubber.[44,45]

The loss factor (tan δ) versus temperature curves for both LNR-UPR and LENR-UPR are presented in Figure 10(c,d), respectively. The neat UPR displayed a single well-defined relaxation peak around 94°C, which is its glass transition temperature. On elastomer addition, a slight shift of the relaxation peak toward lower temperatures was observed. Since LENR is partially miscible in the resin system, the lowering of T_g is mainly owing to the low modulus of the elastomer. Furthermore, the better adhesion and interaction of LENR with the resin matrix were substantiated from IR spectroscopy, FESEM, and impact strength measurements. Conversely, the significantly lower interaction and miscibility of LNR in the polyester matrix could be seen from the morphology and mechanical performance tests, including impact resistance. The reduction in crosslinking density in the modified systems plays a major role in the shifting of T_g. Phase-separated elastomer domains, formed during the curing of UPR, occupies the space in between the reaction sites, thereby impairing the crosslinking reaction at that particular site. This causes the crosslinking density of cured systems to reduce. Thus, the overall crosslinking density reduces on the incorporation of more rubber.[44,45] This shift of the main relaxation process of the matrix toward lower temperatures could also at least be partially explained by a mechanical coupling effect. Indeed, the lower modulus drop at T_g of the UPR matrix on adding elastomer could induce this shift. An ill-defined relaxation peak corresponding to T_g of the

elastomeric phase was also observed around 0°C for the LENR-modified resin.

Figure 9(e,f) show the temperature dependence of the loss modulus for neat UPR and for all the UPRs modified with various percentages of LNR and LENR. Neat UPR showed an unresolved shoulder centered around 44°C, which is attributed to the secondary relaxation of the styrene units bridging the polyester chains and/or to the relaxation of short-chain segments in the vicinity of the residual fumaric unsaturation.[46,47] The relaxation associated with the T_g of the rubber phase for all the modified UPRs can be clearly seen from the loss modulus curves. It can be seen from [Figures 9(e) and 10(f)] that the T_g of LNR and LENR is around −50 and 3°C, respectively. In this case too, the addition of rubber in both systems caused the main peak to shift to lower temperatures. This is attributed to the partial dissolution of rubber into the UPR network, forming a homogenous UPR-rich phase. It could also be due to the decrease in the crosslinking density of UPR on the incorporation of rubber. The distribution of relaxation times of the UPR matrix becomes broader with the inclusion of more rubber. The obtained values from DMA are furnished in Table V.

Thermal Analysis

Thermal stability and degradation behavior of the neat UPR and modified UPRs, with different LNR and LENR contents, were determined from TGA measurements and the results are presented in Figure 10. Thermographs for both the modified systems displayed a single-step decomposition behavior [Figure 10(a,c)]. It is interesting to note that, the thermal stability of rubber-modified UPR was lower than neat UPR regardless the nature of the rubber phase with unsaturated structure which is not contributes in crosslinking. The initial degradation temperature of all samples was around 180°C, and the DTG peak occurred around 380°C [Figure 10(b,d)]. However, from the TGA curves it could be seen that the weight loss started at lower temperatures for samples with higher rubber content. This phenomenon was more marked for LNR-modified UPR blends. The higher thermal stability of LENR–UPR blends is ascribed to the higher compatibility of LENR with UPR, which made it difficult to degrade LENR-UPR blends.

CONCLUDING REMARKS

UPRs have been modified with two types of reactive NR, namely, LNR and LENR, which were prepared by photochemical degradation of NR and ENR, respectively. Modification with both the LNRs significantly improved the mechanical properties of the unsaturated polyester. Morphological studies reveal that the size of the LNR particles increased with increasing rubber content. However, the size of LENR particles was independent of rubber concentration, a behavior unique to LENR. Although the addition of only 1.5 wt % rubber resulted in high tensile strength for both LENR- and LNR-modified UPR, LENR-modified UPR showed higher values for the tensile strength, which could be due to the good compatibility of LENR with the matrix owing to chemical bonding. Impact strength increased about by 154% on increasing the LENR content to 4.5 wt %. However, LNR-modified UPR did not show any significant improvement in the tensile strength. The maximum fracture toughness and fracture energy were observed at 1.5 and 4.5% of LNR and LENR, respectively. Dynamic mechanical analysis of the blends showed two T_gs corresponding to the modified polyester and the rubber phase. The T_g values of both the modified polyesters shifted to lower temperatures on incorporation of the rubber owing to the lower crosslinking density of the blends. The storage modulus of the modified polyesters showed the highest values at 1.5 wt % of rubber. Finally, the LENR-modified polyester showed a better mechanical performance compared to the LNR-modified polyester.

ACKNOWLEDGMENTS

The authors would like to acknowledge the financial support of the Ministry of Higher Education (MOHE) for the FRGS grant UKM-ST-07-FRGS0041-2009 and UKM-DIP-2011-2013. In addition, the authors would also like to thank the French Embassy in Kuala Lumpur for providing financial support (French Scholars in Malaysia).

REFERENCES

1. Auad, M. L.; Frontini, P. M.; Borrajo, J.; Aranguren, M. I. *Polymer* **2001**, *42*, 3723.
2. Barcia, F. L.; Amaral, T. P.; Soares, B. G. *Polymer* **2003**, *44*, 5811.
3. Pham, S.; Burchill, P. J. *Polymer* **1995**, *36*, 3279.
4. Kong, J.; Tang, Y.; Zhang, X.; Gu, J. *Polym. Bull.* **2008**, *60*, 229.
5. Thomas, R.; Abraham, J.; Thomas, P. S.; Thomas, S. *J. Polym. Sci.* **2004**, *42*, 2531.
6. Nam, H. K.; Ho, S. K. *J. Appl. Polym. Sci.* **2005**, *98*, 1663.
7. Ramos, V. D.; Da Costa, H. M.; Soares, V. L. P.; Nascimento, R. S. V. *Polym. Test.* **2005**, *24*, 387.
8. Tripathi, G.; Srivastava, D. *Mater. Sci. Eng.* **2008**, *496*, 483.
9. Thomas, R.; Ronkay, F.; Czigany, T.; Cvelbac, U.; Mozetic, M.; Thomas S. *J. Adhes. Sci. Technol.* **2011**, *25*, 1747.
10. Thomas, R.; Sinturel, C.; Pionteck, J.; Puliyalil, H.; Thomas, S. *Ind. Eng. Chem. Res.* **2012**, *51*, 12178.
11. Robinette, E.; Ziaee, S.; Palmese, G. *Polymer* **2004**, *45*, 6143.
12. Fakhar, A.; Aabaadiaan, M.; Keivani, M.; Langari, A. *World Appl. Sci. J.* **2012**, *20*, 259.
13. Chikhi, N.; Fellahi, S.; Bakar, M. *Eur. Polym. J.* **2002**, *38*, 251.
14. Youssef, M. H.; Mansour, S. H.; Tawfik, S. Y. *Polymer* **2000**, *41*, 7815.
15. Kwanming, K.; Kilnpituksa, P.; Waehamad, W.; Songklanakarin, J. *Sci. Technol.* **2008**, *31*, 4955.
16. Abdullah, I. *Malayisan Pat. MY-110733-A* (**1996**).
17. Abdullah, I.; Zakaria, Z. *Sains Malaysiana* **1989**, *18*, 99.
18. Abdullah, I.; Ahmad, S.; Sulaiman, C. S. *J. Appl. Polym. Sci.* **1995**, *58*, 1125.
19. Phinyocheep, P.; Duangthong, S. *J. Appl. Polym. Sci.* **2000**, *78*, 1478.
20. Abdullah, I.; Ahmad, S. *J. Appl. Polym. Sci.* **1992**, *16*, 353.

21. Ahmad, S.; Abdullah, I.; Sulaiman, C. S.; Kohjiya, S.; Yoon, J. R. *J. Appl. Polym. Sci.* **1994**, *51*, 1357.
22. Tanaka, Y.; Sakaki, T.; Kawasaki, A.; Hayashi, M.; Kanamaru, E.; Shibata, K. U. S. Pat. 5856600 (**1999**).
23. Burfield, D. R.; Gan, S. N. *Polymer* **1977**, *18*, 607.
24. Gillier-Ritoit, S.; Reyx, D.; Campistron, I.; Laguerre, A.; Pal singh, R. *J. Appl. Polym. Sci.* **2003**, *87*, 42.
25. Thanki, P. N.; Reyx, D.; Campistron, I.; Laguerre, A.; Singh, R. P. *Eur. Polym. J.* **2004**, *40*, 2611.
26. Abdullah, I. In Progress in Pacific Polymer Science 3; Ghiggino, K. P., Ed.; Springer: Berlin Heidelberg, **1994**; Chapter 30, pp 351–365.
27. Mathew, V. S.; Sinturel, C.; George, S. C.; Thomas, S. *J. Mater. Sci.* **2010**, *45*, 1769.
28. Hassan, A.; Hassan, A. A.; Mohd Rafiq, M. I. *J. Reinf. Plast. Compos.* **2011**, *30*, 889.
29. Dahlan, H. M.; Ghani, A. H. *J. Sains Nuklear Malaysia* **1993**, *11*, 11.
30. Pearson, R. A.; Yee, A. F. *J. Mater. Sci.* **1991**, *26*, 3828.
31. Lee, W. H.; Hodd, K. A.; Wright, W. W. In Rubber Toughened Plastic; Riew, C. K., Ed.; American Chemical Society: Washington DC, **1989**, pp 263–287.
32. Pearson, R. A.; Yee, A. F. *Polymer* **1993**, *34*, 3658.
33. Loyens, W.; Groeninckx, G. *Polymer* **2003**, *44*, 4929.
34. Ben Saleh, A. B.; Mohd Ishak, Z. A.; Hashim, A. S.; Kamil, W. A. *J. Phys. Sci.* **2009**, *20*, 1.
35. Ozturk, A.; Kaynak, C.; Tincer, T. *Eur. Polym. J.* **2001**, *37*, 2353.
36. Hisham, S. F.; Ahmad, I.; Daik, R.; Ramli, A. *Sains Malaysiana* **2011**, *40*, 729.
37. Ahmad, I.; Hassan, F. M. *J. Reinf. Plast. Compos.* **2010**, *29*, 2834.
38. Seng, Y. L.; Ahmad, S. H.; Rasid, R.; Noum, S. Y.; Hock, Y. C.; Tarawneh, M. A. *Sains Malaysiana* **2011**, *40*, 679.
39. Thomas, R.; Yumei, D.; Yuelong, H.; Le, Y.; Moldenaers, P.; Weimin, Y.; Czigany, T.; Thomas, S. *Polymer* **2008**, *49*, 278.
40. Ratna, D. *Polymer* **2011**, *42*, 4209.
41. Bucknall, C. B. Toughened Plastics; Applied Science: London, **1977**.
42. Newman, S.; Strella, S. *J. Appl. Polym. Sci.* **1965**, *9*, 2297.
43. Szeluga, U.; Kurzeja, L.; Galina, H. *J. Therm. Anal. Calorim.* **2008**, *29*, 555.
44. Mishra, J. K.; Chang, Y. W.; Choi, N. S. *J. Polym. Eng. Sci.* **2007**, *47*, 863.
45. Thomas, R.; Yumei, D.; He, Y. L.; Yang, L.; Moldenaers, P.; Yang, W. M.; Czigany, T.; Thomas, S. *Polymer* **2007**, *48*, 1695.
46. Ragosta, G.; Bombace, M.; Martuscelli, E.; Musto, P.; Russo, P.; Scarinzi, G. *J. Mater. Sci.* **1999**, *34*, 1037.
47. Lenk, R. S.; Padget, J. C. *Eur. Polym. J.* **1975**, *11*, 327.